Progress In Electromagnetics Research Letters, Vol. 53, 121–126, 2015

A Novel Dumbbell-Shaped Defected Ground Structure with Embedded Capacitor and Its Application in Low-Pass Filter Design

Zhi-Yong Chen[1], Lin Li[2, *], and Si-Si Chen[2]

Abstract—A novel dumbbell-shaped defected ground structure (DB-DGS) with embedded capacitor is presented in this paper. Compared with conventional DB-DGS structure, the proposed DB-DGS exhibits many attractive characteristics including double resonance, high Q value and compact size. The equivalent lumped circuit model for the novel DGS is developed, and its parameters are extracted. Based on this new DB-DGS, a low-pass filter (LPF) using the novel DB-DGS has been constructed, which provides a more steep rejection property, a wider stopband and compact size. The proposed structure is experimentally verified through the demonstration of a low-pass filter design.

1. INTRODUCTION

Defected ground structures (DGSs), known as providing rejection of certain frequency band, have been attracting researchers in recent years. They have been presented in a number of different shapes for filter applications [1–4]. Among all these DGSs with different shapes, dumbbell-shaped defect ground structure (DB-DGS) is desirable because of its simple structure and wide stopband [5]. As a result, DB-DGS has been widely used to design compact lowpass filters with wide stopband [6–9]. However, it cannot provide a steep stopband characteristics required by some applications such as elliptic-function LPF owing to its lower Q characteristics. Moreover, its size is still a little large.

In this paper, a novel DB-DGS is presented. By embedding two capacitors in the conventional DB-DGS, the proposed DB-DGS exhibits many attractive characteristics including double resonance, high Q value and compact size. Moreover, the theoretical analysis based on the equivalent LC-circuit model is also carried out to describe the response of the new DGS and also provides an effective guidance in design the proposed DGS. Finally, a low-pass filter has been optimally designed and implemented to illustrate the validity of the proposed DGS.

2. THE NOVEL DEFECTED GROUND STRUCTURE

The schematic diagram of the proposed DB-DGS is shown in Figure 1(a). Obviously, the proposed DB-DGS exhibits the same outline as the conventional one. However, in comparison with the conventional DB-DGS, two capacitors are symmetrically embedded into the two defected lattices.

Owing to the introduction of the embedded capacitors, the novel DB-DGS exhibits different resonant characteristics to the conventional DB-DGS and cannot be depicted exactly by the conventional equivalent parallel RLC circuit in Figure 2(a). Figure 2(b) gives the proposed equivalent RLC circuit for the proposed DGS, where the two inductors of L_1 and L_2 represent the inductive effect brought by the two defected areas of S_1 and S_2 between the embedded capacitor and the edge of the DGS unit. The capacitors of C_1 and C_2 describe the capacitive effect of the etched gap below the conductor line and the embedded capacitors, and R_1 depicts the losses resulted from the defected structure.

Received 20 April 2015, Accepted 4 June 2015, Scheduled 16 June 2015

* Corresponding author: Lin Li (lilin_door@hotmail.com).

[1] Department of Communication Engineering, Zhejiang Sci-Tech University, Hangzhou, Zhejiang 310018, China. [2] Department of Electronic Engineering, Zhejiang Sci-Tech University, Hangzhou, Zhejiang 310018, China.

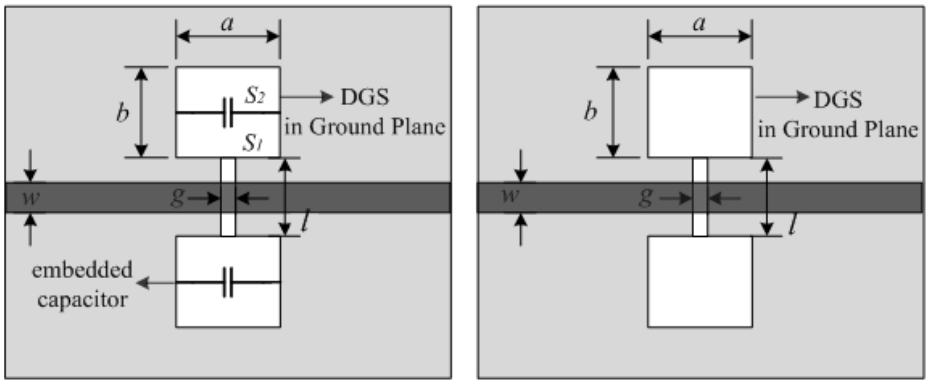

Figure 1. (a) Schematic view of the proposed DGS, (b) schematic view of the conventional DGS. The lattice dimension $a \times b$, the etched gap distance g and the distance l of the two units are set to be 6 mm × 6 mm, 0.6 mm and 5.56 mm, respectively.

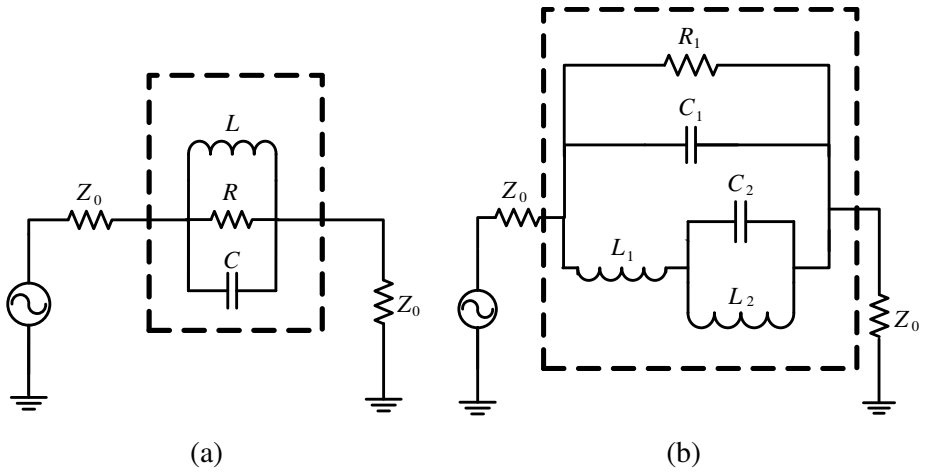

Figure 2. (a) Equivalent circuit of the defected ground structure, (b) equivalent circuit of the defected ground structure with embedded capacitor. The lattice dimension $a \times b$, the distance of etched gap g embedded in DB-DGS are 6 mm × 6 mm and 0.6 mm.

To confirm the validity of the presented equivalent model and compare the transmission characteristics between the conventional and proposed DB-DGSs, both EM and equivalent circuit responses of the two DB-DGSs are all shown in Figure 3. Both the DB-DGSs are built on a 1.5-mm-thick FR-4 substrate with a dielectric constant ε_r of 4.4. And it must be noted that the two exemplary DB-DGSs have the same outline. The dimensions of the two DB-DGS units are listed as follows: $a = 6\,\text{mm}$, $b = 6\,\text{mm}$, $l = 5.56\,\text{mm}$ and $g = 0.6\,\text{mm}$. This study was done by placing a slot under a transmission line 0.286 mm wide. The two capacitors embedded in the proposed DB-DGS are 0.3 pF. The equivalent network extracted parameters of the proposed DB-DGS are: $L_1 = 3.933\,\text{nH}$, $C_1 = 0.304\,\text{pF}$, $L_2 = 2.230\,\text{nH}$, $C_2 = 0.912\,\text{pF}$, $R_1 = 1.5\,\text{k}\Omega$. The equivalent network extracted parameters of the conventional DB-DGS are: $L = 4.836\,\text{nH}$, $C = 0.304\,\text{pF}$, $R = 0.851\,\text{k}\Omega$. Good agreements between the EM and equivalent circuit responses of the proposed DB-DGS can be observed from the graph, indicating the feasibility of the proposed equivalent model.

Firstly, as observed in Figure 3, distinct from the conventional DB-DGS with only one transmission zero, the proposed DB-DGS can generate two transmission zeros.

Thus, the first transmission zero can be employed to sharpen the filter's transition and the second used to extend the stopband, not necessary to introduce another DGS unit with different dimensions. It

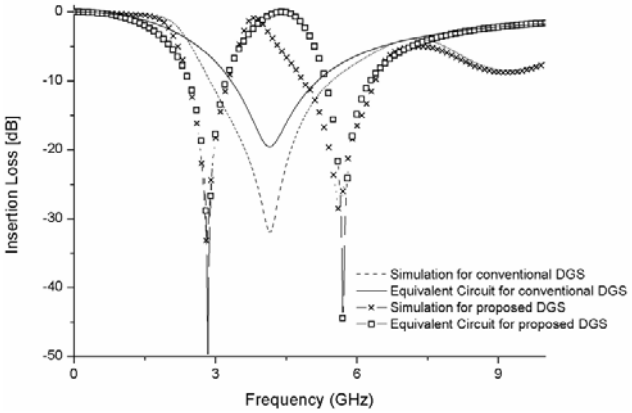

Figure 3. EM simulation and equivalent circuit results of the conventional DGS and the proposed DGS unit with a 3 pF-capacitor.

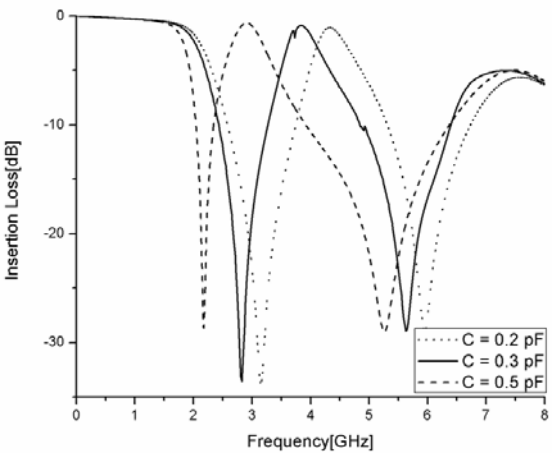

Figure 4. Simulated insertion loss of the novel DGS unit with different embedded capacitor C.

can easily be derived that the frequency of the transmission zeros should satisfy the following equation:

$$f_1 = \frac{1}{2\pi\sqrt{\left(L_1 + \dfrac{L_2}{1 - 4\pi^2 f_1^2 L_2 C_2}\right) C_1}} \tag{1}$$

whose two positive roots are the frequencies of the transmission zeros.

As derived from (1), it is the introduction of C_2 that results in the double resonance.

Furthermore, between the two transmission zeros, the first transmission zero of the proposed structure is only about half as much as that of the convention DGS with the same etched area dimensions. Accordingly, the proposed DB-DGS has much more compact size than the conventional one having the same resonant frequency. This size-reduction effect can be explained using the equivalent circuit in Figure 2(b). Due to the introduction of the embedded capacitors, the parallel circuit of L_2 and C_2 will produce a much larger inductor than L_2 when the frequency is lower than the parallel resonant frequency of L_2 and C_2, and thus push the resonant frequency to the lower side.

Meanwhile, with the reduction of the resonant frequency, the radiation loss is also reduced since the effective radiation caliber has been decreased largely. Thus the proposed DB-DGS exhibits a much larger Q factor than the conventional one. Generally, the Q of the parallel resonant circuit is defined as:

$$Q = \frac{R_0}{\omega_0 L_0} = R_0 \omega_0 C_0 = R_0 \sqrt{\frac{C_0}{L_0}} \tag{2}$$

In the case of the two DGS in Figure 3, the calculated Q factor of the traditional DB-DGS is only 6.704 (resistance R is 851.5 Ω), while the novel DB-DGS provides a high-Q factor of 30.334 (resistance R_1 is 1.5 kΩ). As a result, the cutoff frequency response of the proposed DB-DGS is much sharper than that of the conventional DB-DGS, which means that a higher selectivity can be created.

Moreover, the proposed DB-DGS possesses a very simple mechanism to adjust its frequency response. As shown in Figure 4, the responses of the proposed DB-DGS can be adjusted by simply changing the embedded capacitors. Generally, larger embedded capacitors cause a lower resonant frequency and higher selectivity. And it should be noted that all these adjustment can be fulfilled without the requirements to change the configuration of the DGS, which largely facilitates the filter design.

Finally, it must also be noticed that the proposed structure always cannot provide enough rejection between the two transmission zeros owing to its higher Q. However, as shown in Figure 3, the rejection between the two transmission zeros can be enhanced effectively by the conventional DB-DGS so a filter

with sharpened transition, higher rejection and expanded stopband can be constructed by combining the proposed with conventional DB-DGS.

3. DESIGN AND MEASUREMENT OF A LPF BASED ON THE PROPOSED DGS

Based on the above-mentioned mechanism of the proposed DGS, an exemplary LPF is optimally designed on a 1.5-mm-thick FR-4 substrate. Firstly, the proposed DB-DGS unit is developed. In this design the interdigital structure is employed to realize required capacitor. The proposed DB-DGS with embedded interdigital capacitors is shown in Figure 5. The required capacitor can be obtained by changing the finger width cw, the finger length cl and the coupling distance cg. In this design, the interdigitated structure with $cw = 0.15$ mm, $cg = 0.15$ mm and $cl = 5.5$ mm is used to achieve 0.24 pF capacitance. In Figure 6, the simulated insertion loss of the DGS using embedded lumped capacitor is compared with the same DGS with the proposed interdigital structure. Good agreement can be observed between the two curves, indicating the feasibility of the proposed interdigital structure. And as expected, two transmission zeros at 2.93 GHz and 5.91 GHz appear on the curve.

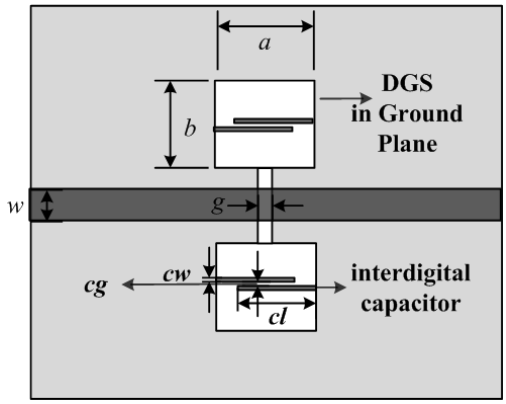

Figure 5. Schematic view of the interdigital capacitor embedded DGS.

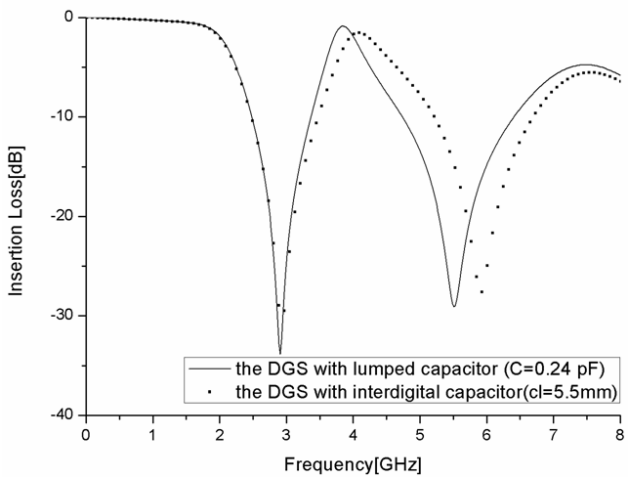

Figure 6. Simulated insertion loss of the DGS with lumped capacitor and the DGS with interdigital capacitor. The value of the lumped capacitor is 0.24 pF and the parameters of interdigital capacitor are: $cl = 0.55$ mm, $cg = 0.15$ mm, $cw = 0.15$ mm.

Furthermore, in order to provide enough rejection between the two resonant frequencies of the proposed DB-DGS, the conventional DB-DGS, whose shape is the same, is also employed in this design. The transmission zero caused by the conventional DGSs is located at 4.19 GHz, which produces rejection between the other two zeros which are behaved by the novel DB-DGS. The LPF is composed of three periodical DB-DGSs — one proposed DB-DGS and two bilateral conventional DB-DGSs. The length of the top connecting microstrip lines between the adjacent DGSs is set to be about quarter-wavelength at the first resonant frequency of the proposed DB-DGS. And it should be noticed that the width of the compensated microstrip line on the top of DGS is broadened to improve the passband match. The layout and photograph of the fabricated filter based on this proposed DB-DGS are shown in Figure 7 and Figure 8, respectively.

The simulated and measured insertion losses of the novel LPF are shown in Figure 9. This LPF has a measured 3 dB cutoff frequency of fc at about 2.20 GHz. The measured passband insertion loss is within 0.5 dB including the SMA connector loss. Because of the great Q characteristics of the novel DGS which is embedded the extra capacitor, the proposed LPF has a terrific deep steepness. With the high-Q factor, the lower attenuation slope is 155 dB/GHz.

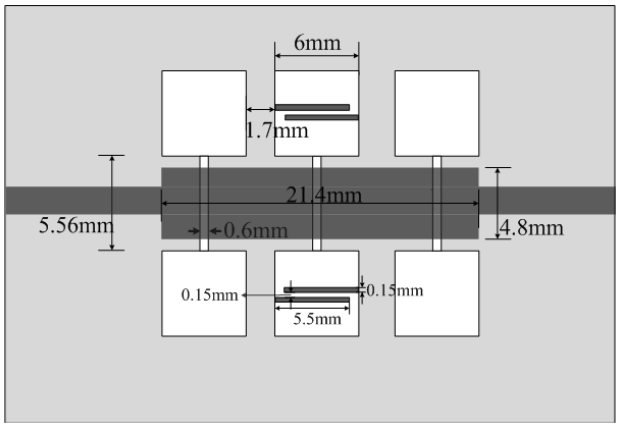

Figure 7. Proposed LPF using the novel DGS.

Figure 8. Fabricated LPF with proposed DGS. (a) Top view, (b) bottom view.

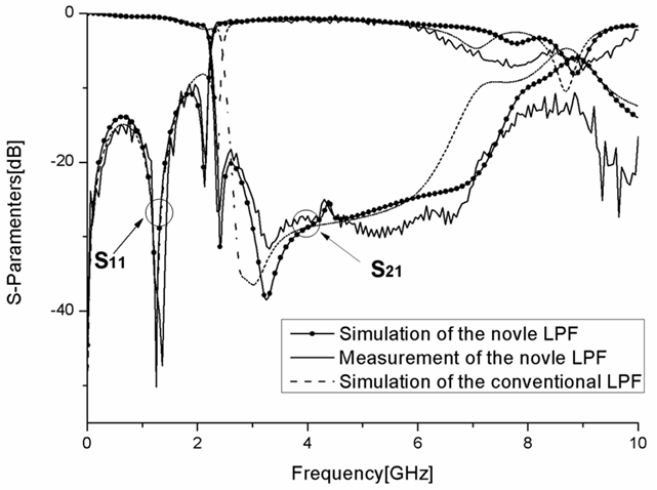

Figure 9. Simulated and measured S-parameter of the novel DGS LPF and conventional DGS LPF.

Table 1. Comparison with the reported LPF.

Parameters\Ref	[1]	[2]	[8]	[9]	This work
Fc (GHz)	1.96	2.86	3.20	3.15	2.20
Stopband 20 dB FBW (%)	236.7	unknown	133	88.9	222.3
No. of zeros	2	2	5	5	4
Attenuation Slope Lower (dB/GHz)	39	12.98	45	275	155
Circuit Size (λ_g^2)	0.019	0.025	0.214	0.200	0.068

With the aid of the second transmission zero produced by the embedded capacitor DGS and the wide stopband characteristics of conventional DGS, the 20 dB rejection stopband is extended from 2.36 GHz (1.073 fc) to 7.25 GHz (3.295 fc) over 20 dB, indicating a very wide 20 dB stopband bandwidth of 2.22 fc. Moreover, these transmission zeros also create a sharp transition for the filter. The attenuation rates at the passband to stopband transition knees are 155 dB/GHz (the measured attenuations being 5 and 31.38 dB at 2.24 GHz and 2.41 GHz, respectively).

In addition, the main circuit of filter has a compact size of 21.4 mm × 17.56 mm, corresponding to $0.068\lambda_g^2$ ($0.288\lambda_g \times 0.236\lambda_g$), where λ_g is the guided wavelength of a 50 Ω transmission line at the central frequency 2.20 GHz.

The comparison of the proposed filter with other reported LPFs is provided in Table 1. Compared with the filters in [1, 2, 8] and [9], the proposed filter has a wide stopband, sharp rejection level and an extremely wide upper passband. Additionally, the size of the filter is much smaller than the reported filters in [1, 2, 8] and [9].

4. CONCLUSIONS

In this paper, a novel DB-DGS with interdigital capacitor is investigated for low-pass filter applications. The basic resonant element of the proposed DB-DGS unit shows the characteristics of elliptic function. Its equivalent lumped RLC circuit model is developed, and its parameters are extracted. The analysis based on the equivalent circuit reveals that the proposed dB-DGS exhibits a much better adjustability of transmission zeros than the conventional dB-DGS. Moreover, the transmission characteristics of the new dB-DGS can be tuned easily by changing the capacitance of interdigital capacitor. Consequently, the proposed dB-DGS has been applied in the low-pass filter design, which provides a more steep rejection property with an improved Q factor. The measured results of the fabricated LPF demonstrate that the novel DGS improves the DB-DGS characteristics performance and enlarges the range of dB-DGS applications. And the results of the equivalent circuit, EM simulation and measurement have a good agreement.

ACKNOWLEDGMENT

This work was supported by the program for Zhejiang leading team of science and technology innovation (2011R50004), the National Natural Science Foundation of China under grants (61101052) and 521 talent project of Zhejiang Sci-Tech University.

REFERENCES

1. San, S. and M. K. Man, "A novel defected ground structure for planar circuits," *IEEE Microw. Wireless Compon. Lett.*, Vol. 16, No. 2, 93–95, Feb. 2006.
2. Balalem, A., A. R. Ali, J. Machac, and A. Omar, "Quasi-elliptic microstrip low-pass filters using an interdigital DGS slot," *IEEE Microw. Wireless Compon. Lett.*, Vol. 17, No. 8, 586–588, Aug. 2007.
3. Chen, Q. and J. Xu, "DGS resonator with two transmission zeros and its application to lowpass filter design," *Electron. Lett.*, Vol. 46, No. 21, 1447–1449, Oct. 2010.
4. Abdel-Rahman, A. B., A. K. Verma, and A. Boutejdar, "Control of bandstop response of hi-lo microstrip low-pass filter using slot in ground plane," *IEEE Trans. Microwave Theory Tech.*, Vol. 52, No. 3, 1008–1013, Mar. 2004.
5. Kim, C. S., J. S. Park, A. Dal, and J. B. Lim, "A novel 1-D periodic defected ground structure for planar circuits," *IEEE Microw. Guided Wave Lett.*, Vol. 10, No. 4, 131–133, Apr. 2000.
6. Dal, A., J. S. Park, C. S. Kim, J. Kim, Y. X. Qian, and T. Itoh, "A design of the low-pass filter using the novel microstrip defected ground structure," *IEEE Trans. Microwave Theory Tech.*, Vol. 49, No. 1, 86–93, Jan. 2001.
7. Lim, J. S., C. S. Kim, D. Ahh, Y. C. Jeong, and S. Nam, "Design of low-pass filters using defected ground structure," *IEEE Trans. Microwave Theory Tech.*, Vol. 53, No. 8, 2539–2544, Aug. 2005.
8. Jung, S., Y.-K. Lim, and H.-Y. Lee, "A coupled-defected ground structure lowpass filter using inductive coupling for improved attenuation," *Microw. Opt. Technol. Lett.*, Vol. 50, No. 6, 1541–1543, Jun. 2008.
9. Liu, H.-W., Z.-F. Li, X.-W. Sun, and J.-F. Mao, "An improved 1D periodic defected ground structure for microstrip line," *IEEE Microw. Wireless Compon. Lett.*, Vol. 14, No. 4, 180–182, Apr. 2004.